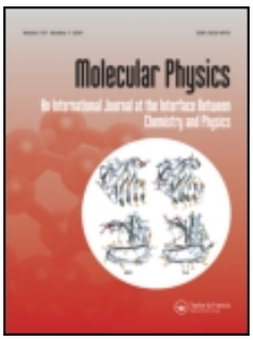

Taylor & Francis
Taylor & Francis Group

Molecular Physics

An International Journal at the Interface Between Chemistry and Physics

ISSN: 0026-8976 (Print) 1362-3028 (Online) Journal homepage: https://www.tandfonline.com/loi/tmph20

Bohm's formulation in imaginary time: estimation of energy eigenvalues

Jian Liu & Nancy Makri

To cite this article: Jian Liu & Nancy Makri (2005) Bohm's formulation in imaginary time: estimation of energy eigenvalues, Molecular Physics, 103:6-8, 1083-1090, DOI: 10.1080/00268970512331339387

To link to this article: https://doi.org/10.1080/00268970512331339387

Molecular Physics, Vol. 103, No. 6–8, 20 March–20 April 2005, 1083–1090

Taylor & Francis
Taylor & Francis Group

Bohm's formulation in imaginary time: estimation of energy eigenvalues

JIAN LIU and NANCY MAKRI*
Department of Chemistry, University of Illinois, 601 S. Goodwin Avenue, Urbana, IL 61801, USA

(*Received 15 September 2004; in final form 29 October 2004*)

Bohm's hydrodynamic formulation of quantum mechanics is employed to solve the diffusion equation. Quantum trajectories are found to behave differently in imaginary time, exhibiting caustic singularities. A wavefunction repartitioning methodology is introduced to prevent the imaginary-time crossing events, leading to stable evolution that does not suffer from the numerical obstacles that characterize Bohmian dynamics in real time. Use of an approximate technique based on trajectory stability properties to solve Bohm's equations in imaginary time leads to an accurate prediction of the energy of a low-lying eigenstate from a single quantum trajectory.

1. Introduction

It is well known that the imaginary-time-dependent Schrödinger equation can be used to generate energy eigenvalues and eigenstates. This is so because imaginary time is mathematically analogous to temperature, and thus propagation along the negative imaginary-time axis quenches the energy of a trial wavefunction, causing it to evolve to the lowest eigenstate of the same symmetry. Quantum Monte Carlo methods [1–3] are powerful implementations of this principle.

The hydrodynamic formulation of quantum dynamics [4–6] was originally developed as an alternative to the Schrödinger equation. Although fully equivalent to the latter, Bohm's approach is a trajectory description. In addition to the standard classical forces exerted on a system by the potential field in which it is embedded, Bohm's trajectories experience an additional 'quantum' force, which is governed by the local curvature of the wavefunction. The density and velocity field from these trajectories satisfy a continuity equation, and thus the Bohmian 'particles' are reminiscent of fluid flow in a space- and time-dependent potential field which itself depends on the detailed characteristics of the flow [7].

Perhaps the greatest appeal of this hydrodynamics formulation of quantum mechanics is its structure in terms of trajectories that satisfy classical-like equations, with a wavefunction expressed in the amplitude-action form familiar from time-dependent semiclassical theory [8, 9]. Unlike the latter, though, the presence of a quantum potential that is to be evaluated from the instantaneous wavefunction density leads to interdependence of the trajectories, making the method non-local and extremely demanding numerically. In spite of significant progress in Bohmian trajectory methodology [10–29], only approximate treatments of bound anharmonic systems have been possible in the past.

In this paper we extend Bohm's formulation to imaginary time. The resulting quantum trajectories satisfy a diffusion equation augmented with Bohm's time-dependent quantum potential. As the imaginary-time parameter increases (in the negative direction) the quantum states described by these trajectories evolve to symmetry-appropriate eigenstates of the Schrödinger equation and the relevant eigenvalue can be extracted from the properties of a single quantum trajectory.

While straightforward in principle, the transformation to imaginary time is accompanied by some subtleties, and the imaginary-time quantum trajectories behave in ways that are entirely different from the well-understood behaviour in real time. The source of these differences is the loss of uniqueness in the amplitude-action decomposition of the imaginary-time wavefunction, which leads to trajectory crossing and the development of 'caustics' that are strictly absent from the real-time formulation. We analyse these behaviours using a harmonic oscillator model and propose a wavefunction repartitioning procedure that entirely eliminates these complications, leading to trajectories that move by very small amounts over the course of the propagation, thus stabilizing the method. The resulting methodology is found to be extremely robust as well as

* Corresponding author. e-mail: nancy.makri@scs.uiuc.edu

Molecular Physics
ISSN 0026–8976 print/ISSN 1362–3028 online © 2005
Taylor & Francis Group Ltd
http://www.tandf.co.uk/journals
DOI: 10.1080/00268970512331339387

stable numerically, suffering from none of the numerical obstacles encountered in real time applications of the Bohmian methodology. While practically all of the available approaches for solving Bohm's equations are easily applicable to the imaginary-time formulation, we implement in the present paper an approximate methodology we recently developed that is based on Bohmian trajectory stability properties (BTS) [28]. This approach offers the advantage of propagating each trajectory based on information contained in its own stability matrix (and its higher-order extensions), thus allowing extraction of the desired energy eigenvalue from the long imaginary-time properties of a single quantum trajectory.

In section 2 we describe the extension of Bohm's equations to the imaginary-time Schrödinger equation and discuss the problems associated with the lack of a unique amplitude-action decomposition and their manifestation as focal points and singularities. We also describe a wavefunction repartitioning procedure that circumvents these problems by effectively implementing the method over short time intervals in which no trajectory crossing occurs. Section 3 reviews the approximate BTS procedure for solving the hydrodynamic equations and brings them in a form suitable for solving the imaginary-time equations with wavefunction repartitioning. Several numerical applications of the method are given in section 4, including strongly anharmonic one-dimensional model systems and three-dimensional Hamiltonians describing the internal dynamics of prototype triatomic molecules. A final discussion is given in section 5, along with some concluding remarks.

2. Bohm's formulation in imaginary time

In real time, Bohm's description of the time evolution of a wavefunction dynamics takes the form [4, 5]

$$\Psi(x;t) = R(x;t)\,\mathrm{e}^{iS(x;t)/\hbar}. \tag{1}$$

Here, $R(x;t)$ is a real-valued amplitude, and the phase $S(x;t)$ satisfies the quantum Hamilton–Jacobi equation

$$-\frac{\partial S(x;t)}{\partial t} = \frac{1}{2m}\left(\frac{\partial S(x;t)}{\partial x}\right)^2 + V(x;t) + Q(x;t). \tag{2}$$

The latter differs from the ordinary equation of classical mechanics through the presence of a quantum potential proportional to the local wavefunction curvature,

$$\begin{aligned} Q(x;t) &= -\frac{\hbar^2}{2m} R(x;t)^{-1}\frac{\partial^2 R(x;t)}{\partial x^2} \\ &= -\frac{\hbar^2}{8m}\left(2\,\frac{\rho(x;t)\rho''(x;t)}{\rho(x;t)^2} - \frac{\rho'(x;t)^2}{\rho(x;t)^2}\right), \end{aligned} \tag{3}$$

where $\rho(x;t) = R(x;t)^2$ is the local density. The trajectory reaches the position x_t at the time t upon integration of the differential equations

$$\dot{x}_t = m^{-1}p_t, \quad \dot{p}_t = \frac{d}{d\tau}\left(\frac{\partial S(x_t,t)}{\partial x_t}\right) = -V'(x_t) - Q'(x_t). \tag{4}$$

The initial condition for equation (2) is the phase $S_0(x_0)$ of the initial wavefunction at the coordinate x_0, and $p_0 = S_0'(x_0)$. The dynamics of the Bohmian trajectories resembles fluid flow, and the density obeys the following hydrodynamic equation:

$$\frac{\partial \rho(x_t;t)}{\partial t} = -\frac{\partial}{\partial x_t}\left(\rho(x_t;t)\frac{p_t}{m}\right). \tag{5}$$

The above equations uniquely determine the amplitude and phase of the wavefunction, which satisfies exactly the time-dependent Schrödinger equation.

As is well known, the substitution $t \to -i\tau$ ($\tau > 0$) transforms the Schrödinger equation into the diffusion equation

$$-\hbar\frac{\partial}{\partial\tau}\Psi(x;\tau) = \hat{H}\Psi(x;\tau). \tag{6}$$

It is easy to show that any wavefunction propagated under this equation evolves to the lowest eigenstate of the same symmetry. For this reason, the diffusion equation offers a convenient and powerful tool for obtaining low-lying eigenstates of many-particle Hamiltonians, which is generally known as the diffusion Monte Carlo method, a common version of quantum Monte Carlo [3].

A similar transformation to imaginary time is possible within Bohm's hydrodynamic formulation. Indeed, substituting $t \to -i\tau$ ($\tau > 0$), $p \to -ip$ and $S \to -iS$ in equations (2), (4) and (5), one obtains the relations

$$\frac{\partial S(x;\tau)}{\partial\tau} = -\frac{1}{2m}\left(\frac{\partial S(x;\tau)}{\partial x}\right)^2 + V(x;\tau) + Q(x;\tau), \tag{7}$$

$$\dot{x}_\tau = m^{-1}p_\tau, \quad \dot{p}_\tau = \frac{d}{d\tau}\left(\frac{\partial S(x_\tau,\tau)}{\partial x_\tau}\right) = V'(x_\tau) + Q'(x_\tau), \tag{8}$$

$$\frac{\partial \rho(x_\tau;\tau)}{\partial\tau} = -\frac{\partial}{\partial x_\tau}\left(\rho(x_\tau;\tau)\frac{p_\tau}{m}\right). \tag{9}$$

These, along with equation (3) for the quantum potential, govern the propagation of Bohmian particles in imaginary time. The wavefunction is again given in terms S and ρ by the equation

$$\Psi(x;\tau) = R(x;\tau)\,\mathrm{e}^{-S(x;\tau)/\hbar}. \tag{10}$$

All variables (and also the wavefunction) are real-valued in these expressions. Equations (7)–(9) are sufficient to describe the evolution of the wavefunction in imaginary time.

While equations (7)–(9) correctly specify the solution to the imaginary-time Schrödinger equation, the partitioning of the wavefunction in equation (10) is not unique. This is so because the exponential factor in this expression is now real-valued, and thus partitioning the initial condition into amplitude- and action-dependent factors is arbitrary. This situation is to be contrasted with the real-time form of the hydrodynamic formulation given in equations (1)–(5), where the definitions of amplitude and phase are evident as well as unique.

The ambiguity in the factorization of the imaginary-time wavefunction into amplitude and phase components has some bothersome implications, of which the most important is the possibility of trajectory crossing. Such behaviour (which is strictly absent from Bohmian trajectories in real time) is reminiscent of the occurrence of 'caustic' or focal points in time-dependent semiclassical theory [30]. In close analogy to the latter, the onset of crossing in imaginary-time Bohmian trajectories is associated with singularities in the amplitude. These features are clearly illustrated by considering the evolution of a Gaussian wavefunction,

$$\Psi_0(x) = \left(\frac{2\gamma}{\pi}\right)^{1/4} \exp(-\gamma x^2), \tag{11}$$

in a one-dimensional harmonic oscillator Hamiltonian with frequency ω. Choosing the initial condition $R(x;0) = \Psi_0(x)$, $S(x;0) = 0$, solution of Bohm's imaginary-time differential equations for the amplitude and phase leads to the expressions

$$R(x;\tau) = \left(\frac{2\gamma}{\pi}\right)^{1/4} \left(\frac{\alpha^2}{\alpha^2\cosh^2\omega\tau - \gamma^2\sinh^2\omega\tau}\right)^{1/4} \times \exp\left(\frac{-\gamma\alpha^2}{\alpha^2\cosh^2\omega\tau - \gamma^2\sinh^2\omega\tau}x^2\right), \tag{12}$$

$$\exp\left(-\frac{1}{\hbar}S(x;\tau)\right) = \left(\cosh\omega\tau - \frac{\gamma}{\alpha}\sinh\omega\tau\right)^{1/4} \times \exp\left(\frac{\alpha(\gamma^2-\alpha^2)\cosh\omega\tau\sinh\omega\tau}{\alpha^2\cosh^2\omega\tau - \gamma^2\sinh^2\omega\tau}x^2\right), \tag{13}$$

where $a = m\omega/2\hbar$. Multiplying these, one recovers the correct form of the imaginary-time wavefunction,

$$\Psi(x;\tau) = \left(\frac{2\gamma}{\pi}\right)^{1/4} \left(\cosh\omega\tau + \frac{\gamma}{\alpha}\sinh\omega\tau\right)^{-1/4} \times \exp\left(-\alpha\,\frac{\gamma\cosh\omega\tau + \alpha\sinh\omega\tau}{\alpha\cosh\omega\tau + \gamma\sinh\omega\tau}x^2\right). \tag{14}$$

Although equation (14) for the wavefunction is well-behaved, its components given by equations (12) and (13) encounter (for $\gamma > \alpha$) essential singularities and the quantum potential becomes undefined when the imaginary-time parameter satisfies the equation $\alpha\cosh(\omega\tau) - \gamma\sinh(\omega\tau) = 0$. Figure 1 shows a few trajectories (obtained from the above analytic treatment) illustrating this situation, which develop

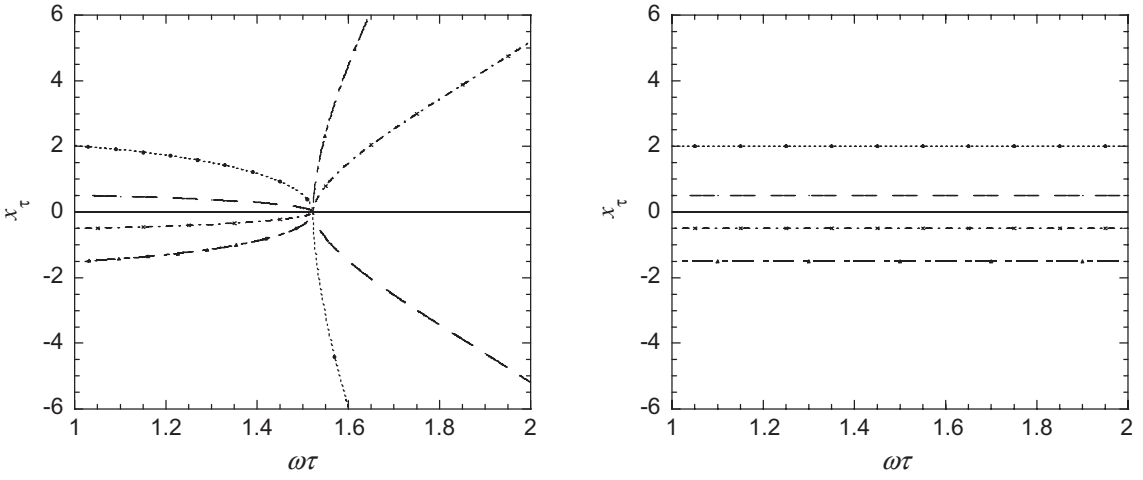

Figure 1. Four imaginary-time Bohmian trajectories corresponding to a Gaussian wavefunction with $\gamma = 1.1\,\alpha$ in a harmonic potential. (*a*) Continuous propagation in time as obtained from the analytic solution of the differential equations. All trajectories are seen to accelerate and eventually go through a focal point when the amplitude and phase develop singularities. (*b*) Trajectories obtained with wavefunction repartitioning. The Bohmian particles remain very close to their initial positions during the propagation.

a caustic at that time. Numerical methods fail as the amplitude becomes exponentially small, and propagation cannot continue past the singular time.

To circumvent these serious difficulties, we exploit the arbitrariness discussed earlier to repartition the wavefunction into amplitude and action parts at the beginning of propagation intervals $\Delta\tau$, such that the amplitude comprises the entire wavefunction (which is always real-valued) and the action equals zero:

$$R(x; n\Delta\tau) \equiv \lim_{\tau \to n\Delta\tau -} \Psi(x; \tau), \quad S(x; n\Delta\tau) = 0. \tag{15}$$

Equation (15) serves as the 'initial' condition for propagation by a time interval $\Delta\tau$, during which

$$\Psi(x; \tau) = R(x; \tau)\, \mathrm{e}^{-S(x;\tau)/\hbar}. \tag{16}$$

This way the effects of the imaginary-time action are incorporated into the density after each step of the procedure. Since the action is reset to zero at the beginning of every propagation step, the momentum of the re-initialized Bohmian trajectories vanishes, causing the particles to move away from their initial position at a very slow rate. This rescaling procedure improves greatly the stability of the propagation.

Finally, the energy associated with an imaginary-time Bohmian trajectory is obtained from the expression

$$E_\tau = -\frac{p_\tau^2}{2m} + V(x_\tau) + Q_\tau(x_\tau). \tag{17}$$

3. Solution of the imaginary-time Bohmian equations

We solve the Bohmian equations of motion approximately, using the BTS procedure we developed recently [28]. This method avoids the use of numerical derivatives in the evaluation of the quantum potential, exploiting instead information encoded in the stability properties of an individual trajectory. As a result, approximate Bohmian trajectories may be propagated one at a time, eliminating the need for data storage that scales exponentially with the number of particles. The initial conditions of the BTS trajectories may be selected by a Monte Carlo procedure. Test calculations have shown that the BTS formulation of certain observables may converge extremely rapid. The approximate nature of the BTS methodology arises from the need to truncate an infinite hierarchy of equations. We have shown that even the lowest-order BTS scheme (where the quantum potential is locally truncated at the second order) is capable of accounting for tunneling effects amounting to several orders of magnitude, and can reproduce rate constants with slightly higher accuracy than possible by quasiclassical methods at a fraction of the computational cost, while improved results can be obtained by retaining higher-order terms.

Below we summarize the BTS procedure in the context of imaginary-time propagation. Following our earlier work, the derivatives of the density required to obtain the quantum potential can be expressed in terms of derivatives of the initial density by repeated differentiation of the continuity equation:

$$\rho(x_\tau) = \rho_0(x_0)\frac{\partial x_0}{\partial x_\tau}, \tag{18}$$

$$\rho'_\tau(x_\tau) = \rho'_0(x_0)\left(\frac{\partial x_0}{\partial x_\tau}\right)^2 + \rho_0(x_0)\frac{\partial^2 x_0}{\partial x_\tau^2}, \tag{19}$$

$$\rho''_\tau(x_\tau) = \rho''_0(x_0)\left(\frac{\partial x_0}{\partial x_\tau}\right)^3 + 3\rho'_0(x_0)\frac{\partial x_0}{\partial x_\tau}\frac{\partial^2 x_0}{\partial x_\tau^2} + \rho_0(x_0)\frac{\partial^3 x_0}{\partial x_\tau^3}, \tag{20}$$

$$\begin{aligned}\rho_0^{(3)}(x_\tau) &= \rho_0^{(3)}(x_0)\left(\frac{\partial x_0}{\partial x_\tau}\right)^4 + 6\rho''_0(x_0)\left(\frac{\partial x_0}{\partial x_\tau}\right)^2\frac{\partial^2 x_0}{\partial x_\tau^2} \\ &\quad + \rho'_0(x_0)\left(4\frac{\partial x_0}{\partial x_\tau}\frac{\partial^3 x_0}{\partial x_\tau^3} + 3\left(\frac{\partial^2 x_0}{\partial x_\tau^2}\right)^2\right) + \rho_0(x_0)\frac{\partial^4 x_0}{\partial x_\tau^4},\end{aligned} \tag{21}$$

etc. The derivates of the initial density are assumed known. Equations (18)–(21) require knowledge of derivatives of the coordinate x_τ reached by a quantum trajectory with respect to its initial condition x_0. The first of these derivatives is related to one of the elements of the stability matrix:

$$\mathbf{M}_\tau = \begin{pmatrix} \dfrac{\partial x_\tau}{\partial x_0} & \dfrac{\partial x_\tau}{\partial p_0} \\ \dfrac{\partial p_\tau}{\partial x_0} & \dfrac{\partial p_\tau}{\partial p_0} \end{pmatrix}. \tag{22}$$

This matrix satisfies the differential equation

$$\frac{\mathrm{d}}{\mathrm{d}\tau}\mathbf{M}_\tau = \mathbf{T}_\tau \cdot \mathbf{M}_\tau, \tag{23}$$

where

$$\mathbf{T}_\tau = \begin{pmatrix} 0 & m^{-1} \\ V''_{\mathrm{tot}} & 0 \end{pmatrix}. \tag{24}$$

In the last equation, $V_{\mathrm{tot}}(x_\tau) = V(x_\tau) + Q(x_\tau)$ is the sum of the classical and quantum potentials acting on the Bohmian particle.

Repeated differentiation of equation (23) with respect to x_0 leads to the following differential equations:

$$\frac{\mathrm{d}}{\mathrm{d}\tau}\frac{\partial \mathbf{M}_\tau}{\partial x_0} = \mathbf{T}_\tau \cdot \frac{\partial \mathbf{M}_\tau}{\partial x_0} + \frac{\partial \mathbf{T}_\tau}{\partial x_0} \cdot \mathbf{M}_\tau, \tag{25}$$

$$\frac{\mathrm{d}}{\mathrm{d}\tau}\frac{\partial^2 \mathbf{M}_\tau}{\partial x_0^2} = \mathbf{T}_\tau \cdot \frac{\partial^2 \mathbf{M}_\tau}{\partial x_0^2} + 2\,\frac{\partial \mathbf{T}_\tau}{\partial x_0} \cdot \frac{\partial \mathbf{M}_\tau}{\partial x_0} + \frac{\partial^2 \mathbf{T}_\tau}{\partial x_0^2} \cdot \mathbf{M}_\tau, \tag{26}$$

etc., which can be solved to yield the higher-order derivatives contained in equations (18)–(21). These equations require knowledge of derivatives of $V''_{\mathrm{tot}}(x_\tau)$with respect to its initial position x_0 which can once again be expressed in terms of stability matrix elements and their derivatives. For example,

$$\frac{\partial V''_{\mathrm{tot}}(x_\tau)}{\partial x_0} = V^{(3)}_{\mathrm{tot}}(x_\tau)\left(\frac{\partial x_\tau}{\partial x_0}\right), \tag{27}$$

$$\frac{\partial^2 V''_{\mathrm{tot}}(x_\tau)}{\partial x_0^2} = V^{(4)}_{\mathrm{tot}}(x_\tau)\left(\frac{\partial x_\tau}{\partial x_0}\right)^2 + V^{(3)}_{\mathrm{tot}}(x_\tau)\left(\frac{\partial^2 x_\tau}{\partial x_0^2}\right). \tag{28}$$

To implement the rescaling procedure described in section 2, one must redistribute the density and its derivatives at regular intervals. We choose the rescaling interval $\Delta\tau$ equal to the propagation imaginary-time step. Defining the density and action at $\tau = n\Delta\tau$ as ρ_n and S_n, respectively, the rescaling procedure for propagation of a particle initially located at x_0 consists of the following operations:

$$\rho_0(x_0; 0) = \Psi_0(x_0)^2, \quad S_0(x_0) = 0, \quad p_0(x_0) = 0, \tag{29}$$

$$\rho_n(x_{n\Delta\tau}; n\Delta\tau) = \rho_{n-1}(x_{n\Delta\tau}; n\Delta\tau)\,\mathrm{e}^{-2S_{n-1}(x_{n\Delta\tau}; n\Delta\tau)/\hbar}, \tag{30}$$

$$S_n(x_{n\Delta\tau}; n\Delta\tau) = 0, \quad p_n(x_{n\Delta\tau}; n\Delta\tau) = 0, \tag{31}$$

$$\begin{aligned}\rho'_n(x; n\Delta\tau) &= \left(\rho'_{n-1}(x; n\Delta\tau) - 2\hbar^{-1}\rho_{n-1}(x; n\Delta\tau)p_{n-1}(x; n\Delta\tau)\right)\\ &\quad\times \mathrm{e}^{-2S_{n-1}(x; n\Delta\tau)/\hbar},\end{aligned} \tag{32}$$

$$\begin{aligned}\rho''_n(x; n\Delta\tau) = \big(&\rho''_{n-1}(x_{n\Delta\tau}; n\Delta\tau) - 4\hbar^{-1}\rho'_{n-1}(x_{n\Delta\tau}; n\Delta\tau)\\ &\times p_{n-1}(x_{n\Delta\tau}; n\Delta\tau)\\ &+ 4\hbar^{-2}\rho_{n-1}(x_{n\Delta\tau}; n\Delta\tau)p_{n-1}(x_{n\Delta\tau}; n\Delta\tau)^2\\ &-2\hbar^{-1}\rho_{n-1}(x_{n\Delta\tau}; n\Delta\tau)p'_{n-1}(x_{n\Delta\tau}; n\Delta\tau)\big)\\ &\times \mathrm{e}^{-2S_{n-1}(x_{n\Delta\tau}; n\Delta\tau)/\hbar}.\end{aligned} \tag{33}$$

The required momentum derivatives are calculated from the stability matrix elements by using the chain rule. Equations (29)–(33) supplement the BTS equations, implementing the wavefunction repartitioning discussed in section 2 that circumvents numerical problems associated with rapidly accelerating trajectories and the emergence of singularities.

Extension of the imaginary-time BTS procedure to many dimensions is (at least in principle) straightforward. For a system of n degrees of freedom, truncation of the BTS hierarchy at the mth order gives rise to $2n + 4n^2(1 + n + n^2 + \cdots + n^{m-1}) + 2$ equations. Storage of the largest array stores n^{m+2} elements.

In the next section we implement the BTS methodology in imaginary time to estimate the ground and first excited state energies of several model and small molecular systems. Results are obtained from a single imaginary-time BTS trajectory. The differential equations are solved using a simplified predictor-corrector algorithm.

4. Model calculations

4.1. *Harmonic potential*

In the case of a harmonic system the quantum potential remains quadratic at all times and Gaussian wavepackets remain Gaussian. As a consequence, the second-order BTS scheme reproduces the ground state exactly. All BTS trajectories yield the precise value of the ground state energy.

Similar remarks pertain to the first excited state eigenvalue of a harmonic oscillator.

4.2. *Quartic potential*

The second model is described by the potential $V(x) = 0.5x^2 + x^4$. This potential is extremely anharmonic: its zero point energy is equal to 0.8038 (i.e. exceeds the harmonic value by 60%) and the spacing between ground and first excited states is 1.9341 (almost double the value of the harmonic term). To estimate the ground state energy we choose a Gaussian initial state of the form $\Psi(x; 0) = (2\gamma/\pi)^{1/4}\mathrm{e}^{-\gamma(x-\lambda)^2}$. We found that BTS trajectories positioned initially near the potential minimum, where the density is maximum, lead to most accurate energy estimates. For the first excited state energy our initial (trial) function has the form $\Psi(x; 0) = (2\gamma/\pi)^{1/4}x\,\mathrm{e}^{-\gamma x^2}$. Again, initial conditions near the maximum density of the first excited state give very accurate results.

For a given initial position of the Bohmian particle, the obtained eigenvalue is independent of the width and centre of the initial wavefunction. The lack of sensitivity to the choice of initial wavefunction is demonstrated very clearly in figures 2 and 3, which show the evolution

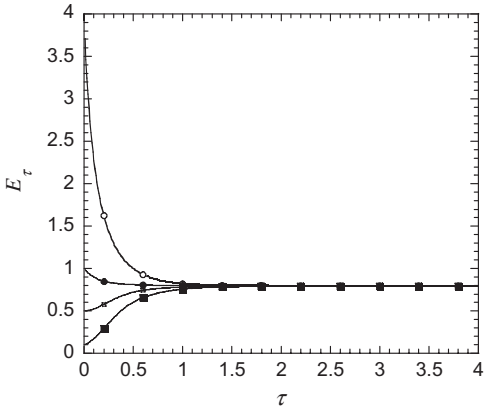

Figure 2. Evolution of lowest energy eigenvalue for a particle originating at $x_0 = 0$ with initial Gaussian wavepackets centred at $\lambda = 0$: (■) $\gamma = 0.2$; (□) $\gamma = 1$; (●) $\gamma = 2$; (○) $\gamma = 8$.

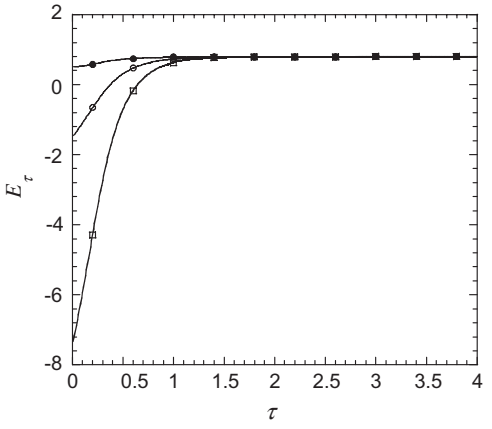

Figure 3. Evolution of lowest energy eigenvalue for a particle propagated from initial Gaussian wavepackets with width $\gamma = 1$. The initial position of the particles is $x_0 = 0$: (□) $\lambda = 4$; (○) $\lambda = 2$; (■) $\lambda = 0$.

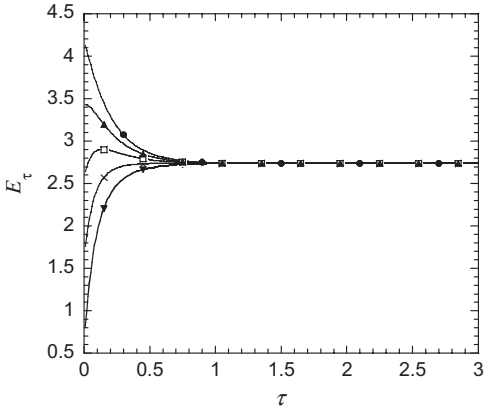

Figure 4. Evolution of first excited state energy eigenvalue for different Bohmian particles propagated from the same initial wavepacket with width $\gamma = 2$ centred at $\lambda = 0$: (▼) $x_0 = -0.5$; (×) $x_0 = -0.6$; (□) $x_0 = -0.7$; (▲) $x_0 = -0.8$; (●) $x_0 = -0.9$.

of the desired eigenvalues for several choices of the wavepacket width and centre. Further, the energy eigenvalues obtained from Bohmian particles with different initial positions agree with one another quite well as long as these particles are placed near the density maximum of the same eigenstate, as shown in figure 4. The stability and robustness of the algorithm shown demonstrated in figures 2–4 on a very strongly anharmonic system is noteworthy and encouraging.

The energy eigenvalues estimated from the imaginary-time BTS procedure (truncated at the sixth order) are shown in table 1 and compared with accurate results obtained from a basis set calculation. We note again that the harmonic values are 0.5 and 1.5, such that the anharmonicity amounts to a correction of the first excited state energy of over 80%. Still, the sixth-order imaginary-time BTS procedure captures this correction extremely well, giving an estimate that is within 0.02% of the exact value.

4.3. *Morse potential for H_2 vibration*

The potential describing the vibration of the H_2 molecule is well described by the Morse form $V(x) = D(1 - e^{-\alpha x})^2$, where $D = 0.1745$ a.u. and $\alpha = 1.026$ a.u. The reduced mass of the molecule is $m = 1837/2$ a.u. Results from fourth- and sixth-order imaginary-time BTS calculations for the ground state energy are shown in table 2 and compared with those from accurate basis set calculations and the harmonic

Table 1. Ground and first excited state energies for the quartic oscillator described in section 4.2.

	Ground state	First-excited state
BTS trajectory initial position	0	0.7
Basis set calculation	0.8038	2.7379
Harmonic approximation	0.50	1.50
Fourth imaginary-time order BTS calculation	0.8356	2.7425
Sixth imaginary-time order BTS calculation	0.7928	2.7375

Table 2. Ground state energies for the Morse oscillator with parameters corresponding to H_2 vibration.

	E_0 (a.u.)
Basis set calculation	0.0098565
Harmonic approximation	0.010
Fourth imaginary-time BTS calculation	0.0098643
Sixth imaginary-time BTS calculation	0.0098567

approximation. Anharmonicity corrections are small in this case, amounting to about 1.5% of the ground state energy. It is seen that the fourth-order imaginary-time BTS method captures the bulk of these corrections, resulting in an energy that is within 0.1% of the exact result. When carried to sixth order the error of the imaginary-time BTS procedure drops to 0.002%.

4.4. *Two-dimensional model for HCN vibrations*

Below we apply the imaginary-time BTS method to a molecular Hamiltonian consisting of the two bending vibrations of the HCN molecule. The potential is expressed in dimensionless normal mode coordinates in the form

$$V = \sum \frac{1}{2}\omega_i q_i^2 + \sum k_{ijk} q_i q_j q_k + \sum k_{ijkl} q_i q_j q_k q_l + \cdots . \tag{34}$$

The potential parameters in the normal coordinate form, which were obtained by transforming the quartic internal-mode force field parameters calculated in [31], are given in table 3. The results of the imaginary-time BTS method are given in table 4.

Table 3. Normal-mode force constants for HCN.

Parameter	Value (cm^{-1})
ω_1	3520.66
ω_3	2230.72
K_{111}	−306.414
K_{113}	−214.569
K_{133}	−56.6978
K_{333}	−103.683
K_{1111}	36.4538
K_{1113}	27.0342
K_{1133}	11.2697
K_{1333}	−7.2678
K_{3333}	6.21578

Table 4. Ground state energies for the two-dimensional Hamiltonian describing the bending vibrations of HCN.

	E_0 (cm^{-1})
Basis set calculation	2861
Harmonic approximation	2875
Fourth imaginary-time BTS calculation	2860
Sixth imaginary-time BTS calculation	2860

4.5. *Three-dimensional model for H_2O vibrations*

The three vibrational modes of H_2O are well described by a quartic force field in normal modes [32]. The potential is again given by equation (34).

Potential anharmonicity in water results in a ∼1% correction to the harmonic estimate for the ground state energy. Results are displayed in table 5. Again, the fourth- and sixth-order imaginary-time BTS calculations capture these deviations from the harmonic approximation very accurately.

Table 5. Ground state energies for the three-dimensional Hamiltonian describing the vibrations of H_2O.

	E_0 (cm^{-1})
Basis set calculation	4652
Harmonic approximation	4712
Fourth imaginary-time BTS calculation	4652
Sixth imaginary-time BTS calculation	4657

5. Concluding remarks

We have adapted Bohm's hydrodynamic formulation of quantum mechanics to the imaginary-time Schrödinger (or diffusion) equation, whose solution allows the determination of energy eigenvalues. Even though the imaginary-time version of the theory does not afford a unique decomposition of the wavefunction into amplitude and action factors, leading to trajectory crossing, the unpleasant consequences of caustics familiar from time-dependent semiclassical approximation, a simple repartitioning technique that we have developed completely circumvents these problems. In addition, the arbitrariness of this decomposition afforded by the real valued solution of the imaginary-time Schrödinger equation allows implementation of the method in a series of short time propagation steps. Because the numerical difficulties associated with essentially all propagation methods develop gradually during the course of the evolution, this repartitioning procedure where all the Bohmian particles are restarted with zero velocity and action at each propagation step circumvents such problems, allowing the extraction of eigenvalues in systems where potential anharmonicity is extremely strong.

Adaptation of the BTS methodology to the imaginary-time Bohmian equations with wavefunction rescaling was shown to be straightforward. In spite of the approximate nature of this method, our test calculations showed that very accurate results are obtainable by carrying through the BTS procedure to fourth or sixth order, even when anharmonic corrections are nearly as large as the eigenvalue spacing. The method appears rather insensitive to the details of the trial wavefunction, requiring only that the Bohmian

trajectory be initialized in the vicinity of a wavefunction maximum. These features are very encouraging, making the imaginary-time BTS methodology with frequent wavefunction repartitioning a potentially powerful tool for the determination of low-lying vibrational or electronic energy eigenvalues. Assessment of the efficiency of this approach in comparison with well-established methods for calculating electronic and vibrational spectra will require additional applications of the method to prototype systems and systematic comparisons.

Acknowledgement

This work was supported by the National Science Foundation under award no. CHE-0212640.

References

[1] W.A. Lester Jr, B.L. Hammond, *A. Rev. phys. Chem.*, **41,** 283 (1990).
[2] M. Suzuk (Ed.), *Quantum Monte Carlo Methods in Condensed Matter Physics*, World Scientific, Singapore (1993).
[3] D.M. Ceperley, L. Mitas, *Adv. Chem. Phys.*, **93,** 1 (1996).
[4] D. Bohm, *Phys. Rev.*, **85,** 166 (1952).
[5] D. Bohm, *Phys. Rev.*, **85,** 180 (1952).
[6] E. Madelung, *Z. Phys.*, **40,** 322 (1926).
[7] P.R. Holland, *The Quantum Theory of Motion*, Cambridge University Press, Cambridge (1993).
[8] J.H. Van Vleck, *Proc. Natn Acad. Sci. USA*, **14,** 178 (1928).
[9] C. Morette, *Phys. Rev.*, **81,** 848 (1952).
[10] B.K. Dey, A. Askar, H. Rabitz, *J. chem. Phys.*, **109,** 8770 (1998).
[11] C.L. Lopreore, R.E. Wyatt, *Phys. Rev. Lett.*, **82,** 5190 (1999).
[12] F.S. Mayor, A. Askar, H.A. Rabitz, *J. chem. Phys.*, **111,** 2423 (1999).
[13] R.E. Wyatt, *Chem. Phys. Lett.*, **313,** 189 (1999).
[14] E.R. Bittner, *J. chem. Phys.*, **112,** 9703 (2000).
[15] R.E. Wyatt, D.J. Kouri, D.K. Hoffman, *J. chem. Phys.*, **112,** 10730 (2000).
[16] D. Nerukh, J.H. Frederick, *Chem. Phys. Lett.*, **332,** 145 (2000).
[17] R.E. Wyatt, E.R. Bittner, *J. chem. Phys.*, **113,** 8898 (2000).
[18] J.C. Burant, J.C. Tully, *J. chem. Phys.*, **112,** 6097 (2000).
[19] C.S. Guiang, R.E. Wyatt, *J. chem. Phys.*, **112,** 3580 (2000).
[20] O.V. Prezhdo, C. Brooksby, *Phys. Rev. Lett.*, **86,** 3215 (2001).
[21] Z.S. Wang, G.R. Darling, S. Holloway, *J. chem. Phys.*, **115,** 10373 (2001).
[22] J.B. Maddox, E.R. Bittner, *J. chem. Phys.*, **115,** 6309 (2001).
[23] I. Burghardt, L.S. Cederbaum, *J. chem. Phys.*, **115,** 10312 (2001).
[24] C.L. Lopreore, R.E. Wyatt, *J. chem. Phys.*, **116,** 1228 (2002).
[25] E. Gindensperger, C. Meier, J.A. Beswick, *J. chem. Phys.*, **116,** 8 (2002).
[26] S. Garashchuk, V.A. Rassolov, *Chem. Phys. Lett.*, **364,** 562 (2002).
[27] Y. Zhao, N. Makri, *J. chem. Phys.*, **119,** 60 (2003).
[28] J. Liu, N. Makri, *J. phys. Chem.* A, **108,** 5408 (2004).
[29] N. Makri, *J. phys. Chem.*, **108,** 806 (2004).
[30] L.S. Schulman, *Techniques and Applications of Path Integration*, Wiley, New York (1981).
[31] U. Wahlgren, J. Pacansky, P.S. Bagus, *J. chem. Phys.*, **63,** 2874 (1975).
[32] A.D. Isaacson, D.G. Truhlar, K. Scanlon, J. Overend, *J. chem. Phys.*, **75,** 3017 (1981).